Postprint of paper published on Journal of Membrane Science 500 (2016) 33-45

Please cite this paper as:

M. Tedesco, C. Scalici, D. Vaccari, A. Cipollina, A. Tamburini, G. Micale, "Performance of the first Reverse Electrodialysis pilot plant for power production from saline waters and concentrated brines", J. Membrane Science 500 (2016) 33–45.

Performance of the first Reverse Electrodialysis pilot plant for power production from saline waters and concentrated brines

Michele Tedesco[a,b], Claudio Scalici[a], Davide Vaccari[a], Andrea Cipollina[a], Alessandro Tamburini[a], Giorgio Micale[a]*

[a] *Dipartimento di Ingegneria Chimica, Gestionale, Informatica, Meccanica (DICGIM), Università di Palermo (UNIPA) – viale delle Scienze Ed.6, 90128 Palermo, Italy.*
[b] *Wetsus, European Centre of Excellence for Sustainable Water Technology, Oostergoweg 9, 8911 MA Leeuwarden, The Netherlands*
[*]*Corresponding author: andrea.cipollina@unipa.it*

Abstract

This work reports experimental data collected for the first time on a full-scale RED pilot plant operated with natural streams in a real environment. The plant – located in the South of Italy – represents the final accomplishment of the REAPower project (www.reapower.eu). A RED unit equipped with almost 50 m^2 of IEMs (125 cell pairs, 44x44 cm^2) was tested, using both artificial and natural feed solutions, these latter corresponding to brackish water (≈0.03 M $NaCl_{equivalent}$) and saturated brine (4-5 M $NaCl_{equivalent}$). A power output up to around 40 W (i.e. 1.6 W/m^2 of cell pair) was reached using natural solutions, while an increase of 60% was observed when testing the system with artificial NaCl solutions, reaching up to ≈65 W (2.7 W/m^2 of cell pair). The unit performance was monitored over a period of five months under, and no significant performance losses were observed due to scaling, fouling or ageing phenomena. Such results are of paramount importance to assess the potential of the technology, towards the successful development on the industrial scale.
A scale-up of the pilot plant is planned through the installation of two additional RED modules, with an expected power output in the order of 1 kW.

Keywords
Salinity Gradient Power; brackish water; brine; natural solutions; REAPower.

1 Introduction

Salinity gradient power (SGP) technologies aim at the exploitation of the energy available when two natural streams with different concentration are mixed together. A number of processes have been proposed so far to capture such renewable energy source: among these, reverse electrodialysis (RED) represents a promising option that might be brought to industrial implementation as soon as new stack components and suitable ion exchange membranes will be available at competitive costs [1,2].

In the RED process, the mixing of concentrated and dilute streams is regulated by a pile of ion exchange membranes (IEMs), which selectively allow the passage of cations and anions, thus generating a net ionic current. This latter is then converted into electric current by means of suitable electrode reactions at the end compartments closing the membranes stack, and finally collected by an external load.

Recently, several experimental works at the laboratory scale have demonstrated that reverse electrodialysis can be suitable for different applications, e.g. for power production from natural salinity gradients [3–9], for waste heat recovery using artificial solutions in a closed loop [10,11], and for wastewater treatment when coupled with electrochemical and biological processes [12,13]. Such experimental investigations notably contributed to understand the fundamental aspects of the RED process. However, the great majority of such works were performed on laboratory-scale RED units, using a relatively small cell pair area (e.g. 10x10 cm^2) and small number of cell pairs (typically 5-10, up to 50 in some cases [8,9]). The only example of a scaled-up unit reported in the literature is a RED stack with 75x25 cm^2 membrane area and 50 cell pairs, which was tested in laboratory conditions with artificial river water and seawater reaching a power output of 16 W (i.e. 0.85 W/m^2 of membrane area) [14,15].

The use of real fresh water and seawater has been recently investigated by Vermaas *et al.* [16], analysing the effect of fouling within laboratory-scale RED units. In that case, a heavy impact of fouling was detected: in particular, a 40% reduction of the power output was observed during the first day of operation, when only a 20 μm filter was used for pre-treatment [16]. The main cause of this performance reduction was attributed to colloidal and organic fouling, which is especially crucial for AEMs, as the fouling layer was composed by large anions (e.g. clay minerals and silica shell of diatoms). The adoption of anti-fouling strategies is therefore necessary to ensure a suitable pre-treatment of natural streams. With this regard, periodic air sparging and switching of feed streams have been proposed as valuable methods to reduce colloidal fouling [17].

In order to further push the development of RED technology, a prototyping and scaling-up phase is now of paramount importance, aiming to shift the target of power production towards the industrial scale. With this regard, the official opening of the first pilot-scale installation in The Netherlands, within the Blue Energy project, was announced in 2014. Such plant is located on the Afsluitdijk, a 32 km-long dyke that separates the IJssel Lake from the Wadden Sea, and is fed with seawater (~28 g/l) and fresh water from the lake (0.2-0.5 g/l). Up to now, no data have been publicly reported since the official opening (November 2014): the only published information was provided by Post *et al.* [14] in 2010, i.e. when the pilot was still in its conceptual design stage. According to the available literature information, the Blue Energy pilot plant in its final configuration will be fed with 220 m^3/h of seawater and fresh water, aiming at the generation of 50 kW gross power output as maximum target.

An interesting alternative to the use of seawater and fresh water as feed streams is the use of concentrated brines in combination with low-concentration saline waters, which allows to further enhance the power outputs of the process [18–20]. As an example, a power density above 6 $W/m^2_{membrane}$ was recently achieved in laboratory investigations using concentrated brines and low-salinity waters as feed solutions [9,20]. In particular, regarding the dilute stream, fresh water can often represent the main contribution to the internal electric resistance of the

stack, thus limiting the power output. Therefore, the use of a low-concentration saline stream instead of fresh water allows to lower the internal stack resistance, though reducing the inlet concentration difference. For this reason, a trade-off has to be identified regarding the optimal value of concentration that reduces the stack resistance without appreciable loss in terms of driving force. This concept was the basis of the REAPower project [21], whose main goal was to demonstrate the potential of reverse electrodialysis technology using saline streams and concentrated brines as feed solutions.
This idea was firstly addressed through modelling works [22] and experimental demonstration at laboratory scale [9,23]. In particular, a process simulator was developed by Tedesco *et al.* [24] to describe the operation of a RED plant fed with such high saline solutions. Investigating the effect of salt concentration on power density for a laboratory RED unit (10cmx10cm cell pair area), optimal feed conditions were identified in the use of brackish water (0.08-0.1 M NaCl) as dilute and brine (4.5-5 M NaCl) as concentrate [24]. Assuming similar feed conditions on a pilot scale, a power output of more than 1 kW was predicted for a plant equipped with 3 RED modules of 44x44 cm^2 and 500 cell pairs [25].
Following these modelling predictions, a demonstration plant was designed and constructed as final accomplishment of the REAPower project. The plant is located within the saltworks of Ettore e Infersa in Marsala (Trapani, Italy): such location provides both feed streams for power production, i.e. brackish water (from a shoreline well) as dilute, and almost saturated brine from saltworks as concentrate (Figure 1).

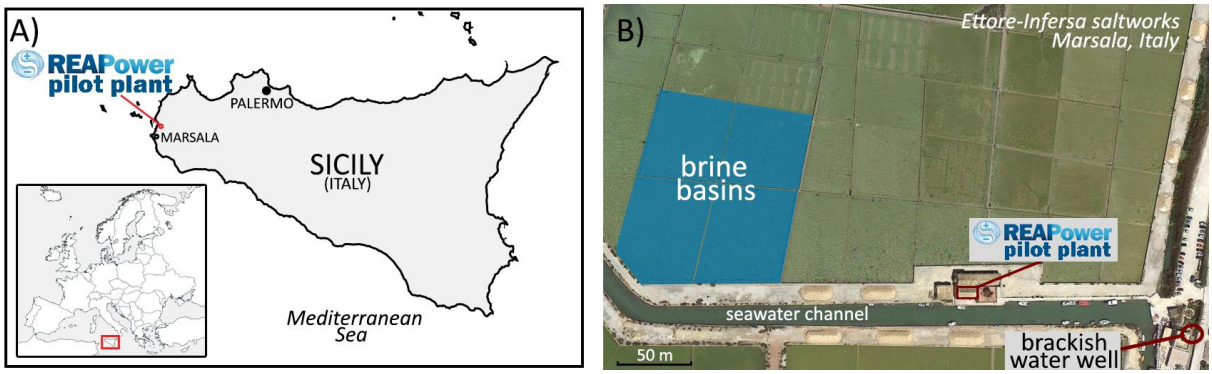

Figure 1. A) Location of the REAPower pilot plant in Marsala (Italy). B) Satellite image of the REAPower plant installation site (*Ettore-Infersa* saltworks, Marsala, Italy). Saturated brine from basins and brackish water from a shoreline well are available in the same area as feed streams for the RED process.

Focus of this work is to present the activities carried out during the design, installation and testing of the 1st phase of the REAPower demonstration plant. A RED unit with 44x44 cm^2 membrane area equipped with 125 cell pairs was installed in such environment and tested both with real solutions (brine and brackish water) and with artificial NaCl solutions. The performance of the plant was monitored over a period of five months of operation, providing for the first time experimental data on a full-scale RED pilot plant operating in a real environment.

2 Plant design and installation

2.1 The installation site

The Ettore-Infersa saltworks in Marsala (Trapani, Italy), situated on the west coast of Sicily (Figure 1.A), is one of the most important areas in the Mediterranean Sea for the production of

sea-salt. With its availability of large amounts of concentrated brines, this site represents a perfect location for demonstrating the feasibility of RED technology with highly concentrated solutions.

A saltworks is a delicate natural environment where sodium chloride is extracted from seawater, exploiting the natural evaporation caused by solar energy and wind. Process waters (starting from seawater) flow along large basins driven by gravity or by low-prevalence pumps. Due to evaporation, salt concentration increases along the basins ending with a brine saturated in NaCl which is used for the final crystallisation process. A careful flow distribution (regulated through small canals and gates) allows to precipitate undesired salts such as calcium sulphates and carbonates in intermediate basins, while sodium chloride crystallises only in the last basins. The final product has a purity in NaCl normally higher than 97% (i.e. food-grade salt) [26].

Clearly, any saltworks area is a feasible location for salinity gradient power production, due to the large availability of seawater and concentrated brine in the same site. In particular, the Marsala saltworks has been selected as installation site thanks also to the presence of brackish water, which is available from a shoreline well (Figure 1.B). It is worth mentioning that, in the present experimental campaign, the use of brine for RED power production does not compromise the salt production process of the saltworks, as the daily volumes required for the RED plant (about 5 m^3/d) are negligible compared to the total volume of the basins (larger than 2000 m^3). Moreover, the slightly depleted brine coming out from the RED plant can be recycled to the basins, where the evaporation rate due to sun and wind (typically between 5 and 10 l/m^2/d, i.e. about 60-120 m^3/d in total for the 4 basins) can rapidly restore the brine concentration, without affecting appreciably the evaporation process. Considering that the 4 dedicated basins constitute only a small percentage of the total crystallisation basins of the saltworks of Trapani and Marsala, a process scale-up of 3-4 orders of magnitude in this site could be still considered technologically feasible and well integrated within the conventional production cycle.

The main characteristics of the feed streams of the plant are reported in Table 1. The available brine has a conductivity ranging between 150-220 mS/cm (i.e. $NaCl_{equivalent}$ concentration up to 4-5 M), according to the period of the year: a saturated solution is available in summer, while the brine is diluted by rainfalls during winter. Conversely, the conductivity of brackish water is rather stable, equivalent to a 0.03 M NaCl solution (Table 1).

Table 1. Characteristics of feed streams of the REAPower plant in Marsala (Italy).

Solution	**Conductivity**	**T**	**Typical ion composition (g/l)** [b]					
	(mS/cm)	**(°C)**	**Na^+**	**K^+**	**Ca^{2+}**	**Mg^{2+}**	**Cl^-**	**SO_4^{2-}**
Brine	150-220 [a]	27 (18-31)	64 (48-94)	11 (7-14)	0.4 (0-1.3)	45 (24-58)	192 (175-219)	39 (0-75)
Brackish water	3.4	24 (17-27)	0.41	0.02	0.27	0.08	1.19	0.11

[a] The brine conductivity changes appreciably during seasons, ranging from 150 mS/cm in winter up to 220 mS/cm in summer.

[b] Brine composition can significantly change along the year: the most representative value of concentration is reported for each species, while the typical range of variation is indicated between brackets.

Table 1 reports also the typical ion composition of brine and brackish water. Apart from Na^+ and Cl^-, other ions are present in considerable concentration in the brine, especially Mg^{2+} and K^+, while brackish water presents a relatively high concentration of Ca^{2+} and SO_4^{2-}.The content of NaCl (expressed as equivalent percentage, considering Na^+ as a limiting species) in brine and brackish water was 47% and 46%, respectively.

Both feed solutions were rather clean, especially brackish water was practically free of suspended matter (as expected, being extracted from a shoreline well). The use of clean feed

streams is a remarkable advantage for the unit operation, determining a lower risk of channel plugging and membrane fouling.
The feed solutions were constantly monitored in terms of electrical conductivity, being the only measurable variable related to salt concentration in online standard measuring systems. Indeed, electrical conductivity can be easily related to the salt concentration in case the solutes composition can be considered stable (as in the case of the brackish water), while it gives only an important, yet qualitative, information when a variability in composition characterises the feed solution (as in the case of saltworks brines).

2.2 Pilot plant description

Feed streams intake

The pilot plant is connected with two intake lines (~200 m long each), one for the concentrated brine from saltworks basins and one for the brackish water from a shoreline well (Figure 1.B). In particular, the concentrated brine is taken from four dedicated basins, containing saturated brine normally adopted for NaCl crystallisation. In addition, two storage tanks (2 m^3 capacity each) were installed for testing the system with artificial (NaCl) solutions.
Both brackish water and brine are firstly sent to a filtration stage, then to a buffer tank (125 l capacity), and finally fed to the RED unit for power generation. The solutions exiting from the RED unit are a slightly diluted brine and a slightly concentrated brackish water: the former can be recycled directly to the saltworks, where its original concentration will be naturally restored by the sun and wind evaporation; the latter is discharged in a seawater channel close to the installation site (Figure 1.B). A simplified scheme of the plant layout is shown in Figure 2.

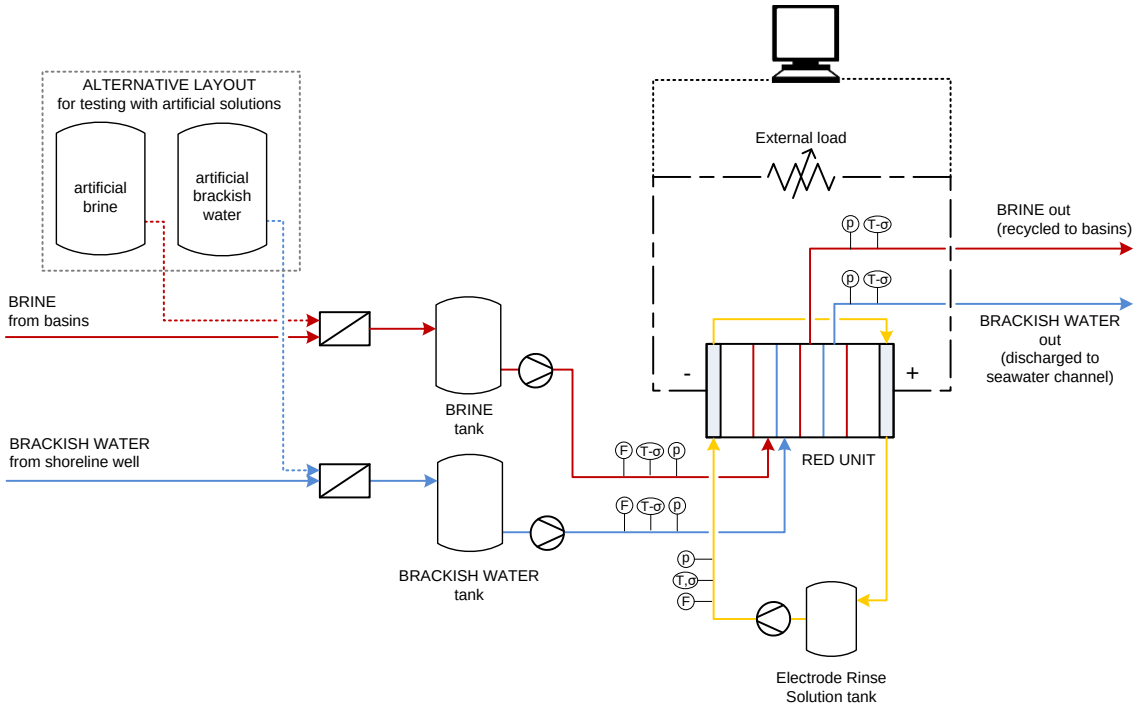

Figure 2. Simplified scheme of the plant layout.

Reverse electrodialysis unit

The installed RED module has a cell pair area of 44x44 cm^2 and is equipped with 125 cell pairs (i.e. 48 m^2 of total membrane area installed). The RED unit, provided by REDstack BV (The Netherlands), is designed for a cross-flow arrangement of the feed solutions, with four segmented electrodes of Ru-Ir oxide coated Ti mesh (Magneto Special Anodes BV, The Netherlands) installed in the external compartments. The stack components are ion exchange membranes purposely developed for highly concentrated solutions (Fujifilm Manufacturing Europe BV, The Netherlands), and 280 µm woven net spacers (Deukum GmbH, Germany). The main properties of the installed membranes are reported in Table 2.

Table 2. Physical properties of Fujifilm ion exchange membranes installed in the REAPower pilot plant*.

Membrane	**Thickness (µm)**	**Permselectivity[a] (-)**	**Electrical resistance[b] (Ω cm^2)**	**Hydraulic permeability (ml/bar h m^2)**	**Ion Exchange Capacity (meq/g)**
AEM RP1 80045-01	120	0.65	1.55	4.96	1.28
CEM RP1 80050-04	120	0.90	2.96	4.72	1.45

* Data provided by the membranes manufacturer.
[a] Permselectivity measured between 0.5 M NaCl – 4 M NaCl conditions at 25°C.
[b] Electrical resistance measured in 0.5 M NaCl solution at 25°C. Adapted from [27].

The electrode rinse solution (ERS) was purposely selected to minimise the environmental impact in the unlikely case of leakage from the electrode compartments into the saline compartments. For this reason, the use of hexacyanoferrate compounds was avoided, although such redox couple has been widely adopted for laboratory-scale investigation of the RED process [28]. Conversely, iron salts ($FeCl_2$/$FeCl_3$) have been identified as suitable redox couple for such delicate environment [29]. Therefore, an aqueous solution of 0.3 M $FeCl_2$, 0.3 M $FeCl_3$

and 2.5 M NaCl as supporting electrolyte was used as electrode rinse solution. A small amount of HCl was added to the ERS to keep the pH in the range of 2-3 and avoid precipitation of iron compounds [30].

Pre-treatment section

Both brackish water and brine were pre-treated through a 50 μm cleanable filter and two cartridge filters of 25 μm and 5 μm. In addition, a shock treatment with sodium hypochlorite was performed (by feeding the stack with a 5 ppm NaClO solution, prepared in the storage tanks for brackish water, twice per week): this allowed to prevent the growth of bio-fouling film in the dilute compartments of the RED unit. The hypochlorite dosing was not necessary for brine, as bio-fouling is already inhibited by the high salt concentration of the solution.

Pumps

Three centrifugal pumps with variable speed (Schmitt MPN 130, Kreiselpumpen GmbH & Co.KG, Germany) were used to feed all solutions (i.e. concentrate, dilute and ERS) to the RED unit.
A centrifugal pump was used to extract the brackish water from the well in order to continuously fill the buffer tank. An immersed pump (centrifugal pump with open impeller) was installed directly in the ponds for the brine intake. The use of such pump – especially suitable for waters with suspended matter – was necessary due to the precipitation of salt within the brine basins occurring in summer months, when the brine reaches the saturation in sodium chloride. In this way, the saturated brine was sucked by the pump along with salt crystals, which were eventually blocked in the pre-filters (though this required frequent washing of the filters).
For testing with artificial feed streams, two membrane pumps (Shurflo SH-4111-03) were adopted for pumping the solutions from the storage vessels to the buffer tanks.

Instrumentation

The measuring instrumentation was constituted by temperature-conductivity sensors/transmitters (Jumo CTI-500) and pressure transducers (Jumo Midas SW) for both inlet and outlet solutions. The inlet flow rate of both concentrate and dilute feed streams was measured by magnetic flowmeters (Khrone IFC 100 C). Likewise, conductivity, temperature and flow rate of the electrode rinse solution were monitored with similar sensors.
All measured signals, along with the voltage difference between the electrodes were collected by a data logger (LabVIEW^{TM}, National Instruments, USA) at a frequency of 1 Hz, while the electric current (I) was measured by an external ampere-meter.
An external load was used during the testing, constituted by a variable resistor (0 – 22 Ω) connected in parallel with five lamps (10 W nominal power). These allowed to have a visual indication of the power generation. Moreover, the presence of lamps in parallel increased the accuracy of the equivalent variable resistor in the range of 1-2 Ω (Figure 3.A), i.e. when the external resistance is equal to the stack resistance and the maximum power is produced (as already demonstrated in previous literature works [8,9]).
The pumps, piping and instrumentation were all installed on a compact supporting structure built with corrosion-resistant materials (PVC sheets and Bosch aluminium profiled bars). The front panel of the supporting structure is shown in Figure 3.B, where all the membrane valves and measurers (conductivity-meters, flowmeters, pressure transducers) are visible.

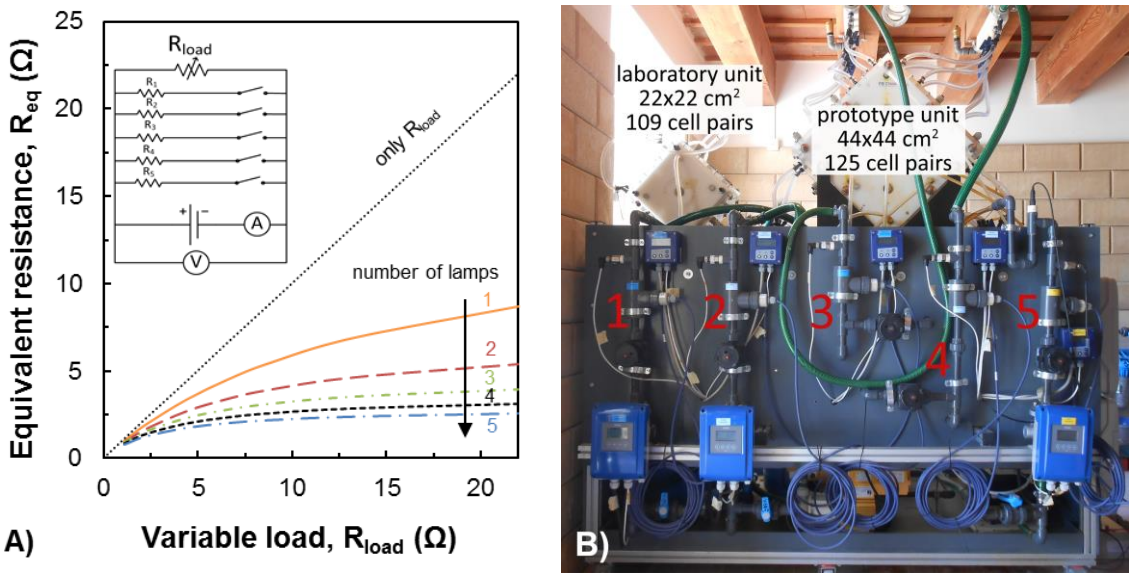

Figure 3. A) Equivalent resistance of the external circuit adopted during the tests. Five lamps (10 W each) were connected in parallel to the variable resistor (R_{load} = 0 – 22 Ω) to increase the accuracy in the range of maximum power output (1 – 2 Ω).
B) Front-end panel of the supporting tray. Five pipelines can be identified: HIGH inlet (1), LOW inlet (2), HIGH outlet (3), LOW outlet (4), ERS (5). Two RED units are shown on the tray for visual comparison: a laboratory stack (about 10 m^2 membrane area) and the RED unit adopted for the experimental campaign.

3 Experimental procedure

The RED prototype was tested both under "constant load" conditions – i.e. connecting the RED unit with a fixed resistance – and under "variable load" conditions, by changing the external resistance in order to study the entire voltage-current (E-I) curve.
Before the measurement, both dilute and concentrate compartments were washed with brackish water for some minutes, ensuring that uniform conditions of flow rate and pressure drops in both compartments were reached. This procedure was necessary to remove the possible channel plugging caused by the precipitation of salt from the saturated brine during stand-by periods. Conversely, the shutdown operations consisted in rinsing both compartments with brine, in order to store the membranes under wet, high-salinity, conditions, thus avoiding membranes drying and preventing the formation of bio-fouling. For long inactivity periods (i.e. days), all the compartments (including electrode compartments) were filled with artificial (NaCl) brine.
During the testing, the stack voltage (E_{stack}) and the external current (I) were directly measured as previously described. Therefore, the power generated by the system (P) can be calculated according to Ohm's law:

$$P = E_{stack}\, I \tag{1}$$

The internal electric resistance (R_{stack}) can be evaluated as the slope of the experimental curve on the E_{stack}-I plot, according to the equation:

$$E_{stack} = OCV - R_{stack}\, I \tag{2}$$

where OCV is the open circuit voltage (i.e. the stack voltage under zero-current condition).
The net power is evaluated from eq. 1 by subtracting the pumping power due to hydraulic losses:

$$P_{net} = P - \frac{\Delta p_{LOW}\ Q_{LOW} + \Delta p_{HIGH}\ Q_{HIGH}}{\eta_{pump}} \tag{3}$$

where Δp are the pressure drops, Q is the volumetric flow rate, and η_{pump} is the pump efficiency (assumed as 75%); subscripts *HIGH* and *LOW* refer to concentrate and dilute compartments, respectively.
Dividing both eq. 1 and 3 by the total cell pair area ($N\ A$), the gross and net power density are obtained:

$$P_d = \frac{P}{N\ A} \qquad\qquad P_{d,net} = \frac{P_{net}}{N\ A} \tag{4, 5}$$

Aside from gross and net power density, other figures of merit have been analysed. The yield of the RED system (Y) can be defined as the amount of net power produced per cubic meter of feed solution:

$$Y = \frac{P_{net}}{Q_{av}} \tag{6}$$

where Q_{av} is the average flow rate of dilute and concentrate. Finally, the energy efficiency is evaluated as the ratio between the power output and the theoretical power obtainable if the concentration equilibrium of the mixed solutions was achieved under a reversible transformation (P_{rev}):

$$\eta = \frac{P}{P_{rev}} \tag{7}$$

The theoretical power is related to the Gibbs free energy of mixing of the two solutions, therefore activity coefficients and molar concentrations of all ions should be taken into account. For the sake of simplicity, NaCl has been assumed as key component of the feed solutions and the reversible power has been estimated as

$$P_{rev} = 2\,R\,T\left(Q_{LOW}\ C_{LOW,in} \ln\frac{\gamma_{LOW,in}\ C_{LOW,in}}{\gamma_{eq}\ C_{eq}} + Q_{HIGH}\ C_{HIGH,in} \ln\frac{\gamma_{HIGH,in}\ C_{HIGH,in}}{\gamma_{eq}\ C_{eq}}\right) \tag{8}$$

where R is the universal gas constant, T is the average temperature of feed solutions, C and γ are the molar concentration and the mean activity coefficient of equivalent NaCl solutions. The equilibrium concentration (C_{eq}) is evaluated as

$$C_{eq} = \frac{Q_{LOW}\ C_{LOW} + Q_{HIGH}\ C_{HIGH}}{Q_{LOW} + Q_{HIGH}} \tag{9}$$

Activity coefficients and NaCl equivalent concentrations were evaluated from the conductivity of both solutions. The relevant correlations are reported in the Appendix.

4 Results and discussion

4.1 Tests with real brackish water and brine

The RED prototype was firstly tested with real brackish water and brine under constant load conditions, in order to investigate the stability of the system when fed with natural solutions.
As a reference test condition, a flow rate of 8 l/min was assumed for both dilute and concentrate, i.e. ideally corresponding to 1 cm/s of fluid flow velocity within the compartments. For the electrode rinse solution, a flow rate of ~3 l/min was used for all tests, ensuring a good trade-off between enhancing the mass transport and avoiding high pressure drops in the electrode compartments.
Results collected during a typical measurement are shown in Figure 4, where the RED unit was connected to a variable external resistance for 1 hour of operation. In particular, all the monitored variables are shown as a function of time.

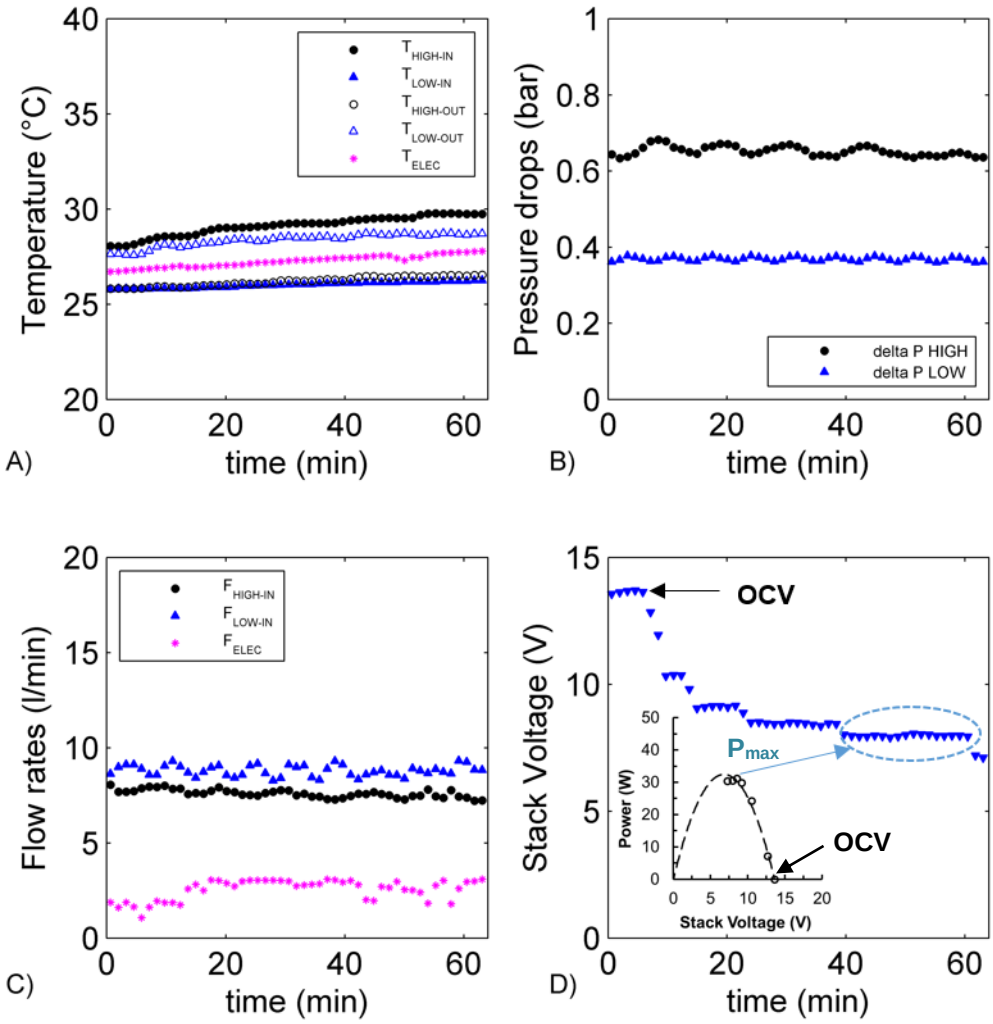

Figure 4. Power measurement using real brackish water (3.4 mS/cm) and brine (187 mS/cm) at 1 cm/s fluid flow velocity (i.e. ~8 l/min feed flow rate). A) Temperature. B) Pressure drops. C) Flow rates. D) Stack voltage. The

resulting power is shown as a function of the stack voltage as inset plot in (D). Flow rate of the electrode rinse solution: 2.6 l/min.

A continuous and stable operation was registered for all variable, but the stack voltage. This latter varied from the maximum value achieved under Open Circuit Voltage (OCV) conditions, i.e. when an infinite external resistance was applied, to a value equal to OCV/2 (obtained when the external resistance matches R_{stack}), corresponding to the condition of maximum power output of the system, being in the present test above 30W (Figure 4.D). It is worth noting that such test was carried out when the temperature of brine in the basins raised up to 28-30°C (late June). Conversely, the temperature of brackish water (coming from a well) was around 26°C. The experimental campaign was carried out during summer months (May 2014 – September 2014). A lower power production is expected during winter period, due to both a lower temperature (15-17°C) and dilution of the brine resulting in lower values of conductivity (e.g. 100-150 mS/cm).
Notably, Figure 4.A shows a crossing of the outlet temperature of solutions, reaching on average 27-28°C and 26°C for brackish water and brine, respectively. A crossing in the outlet temperature (that would not be possible in a co-current configuration) is not surprising in this case, as the RED stack was fed in cross flow arrangement, working similarly to a counter-current configuration [31].
The brackish water compartment showed lower pressure drops than the brine compartment (Figure 4.B) due to both the lower viscosity of the dilute solution and the partial plugging of the spacer-filled channel caused by the likely precipitation of NaCl (though this phenomenon occurred especially when feeding the stack with natural saturated brines).
The RED prototype was tested with real solutions under different conditions of flow rates. Figure 5 shows the effect of increasing flow velocity (both for brackish water and brine) on the power output.

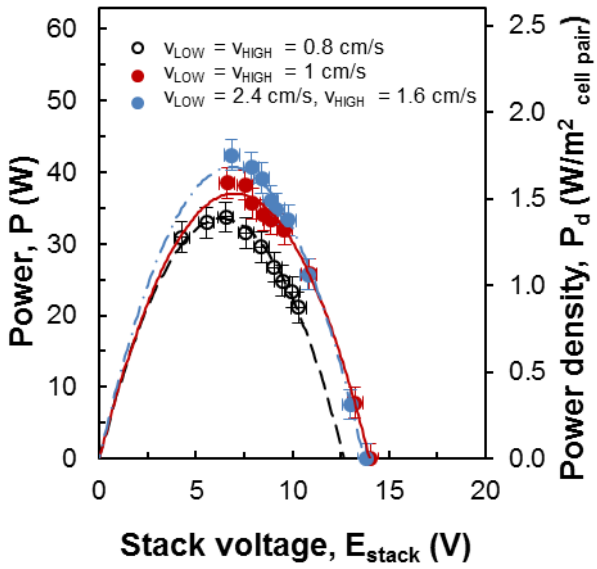

Figure 5. Influence of feed flow velocity on process performance. Power measurements performed feeding the prototype (44x44 cm^2, 125 cell pairs) with real brine (cond. 196 ± 11 mS/cm, $T_{HIGH} \approx 28 \pm 1$ °C) and brackish water (cond. 3.4 ± 0.1 mS/cm, $T_{LOW} \approx 25 \pm 1$ °C).

Increasing the flow velocity can be beneficial in the enhancement of power density for two reasons: 1) reduction of the residence time of solutions inside the stack, leading to higher

driving force and OCV [32]; 2) improved mass transfer phenomena, thus reducing the stack non-ohmic resistance [33–35]. As an overall result, a 30% higher power output was reached by increasing the flow velocity from 0.8 up to 2.4 cm/s (Figure 5). However, in general, a regular trend for OCV and stack resistance as a function of flow velocity was not detected during the experimental campaign with real solutions (see Fig. A.1 provided in the Appendix). In fact, the experimental scattering due to the variability of several operating parameters (e.g. feed temperature, brine composition, reversible salt precipitation occurring in some tests, etc.) tends to hide the weak influence that fluid flow velocity normally has on the process.
It should be also noted that high flow rates lead to a rapid reduction of the net power density and the process efficiency [9,34]. In fact, doubling the flow rate generates an increase in pumping losses by 4-8 times (depending on the laminar/transitional/turbulent regime characterising the flow in the piping, manifolds and RED channel). The second effect is related to the reduction in the residence time and subsequent reduction in the conversion of the available salinity gradient into electricity.
Moreover, maximum values of flow rates for practical applications are limited by the pressure drops, which should generally be kept below values of 1 bar for avoiding mechanical stresses and limit internal leakages. In this case, at the maximum investigated flow rate (Q_{LOW} = 18 l/min, i.e. 2.4 cm/s; Q_{HIGH} = 12 l/min, i.e. 1.6 cm/s), pressure drops were 0.7 and 0.9 bar for dilute and concentrate, respectively. In fact, brine flow velocity higher than 1.6 cm/s was avoided in order to keep the pressure drop below 1 bar, as suggested by the stack manufacturer.

4.2 Tests with artificial solutions

Aside from the operation with real brine and brackish water, the RED system was also tested with artificial solutions.
These were prepared using tap water and sea-salt from the saltworks (purity in NaCl between 95% and 97%) and also with almost pure NaCl (>99.5%). The typical concentration of sea-salt used for tests with artificial solutions is reported in Table 3. As already indicated in paragraph 2.1, the electrical conductivity was selected as a reference variable. For the same reasons, the comparison with artificial solutions was performed keeping the same conductivity as in the case of the real brine (~200-220 mS/cm) and brackish water (3.4 mS/cm). It is worth mentioning that this choice leads to NaCl concentration in the artificial solutions larger than in natural ones, although the overall salt concentration in both cases is similar. A reference case is identified for the system under "feed-controlled" operations, i.e. using artificial NaCl solutions. When passing to natural solution with similar conductivities (and, in facts, adopting a NaCl artificial brine close to saturation as in the case of the natural brine), the detrimental effect on the power generation can be thus observed.
In order to avoid any influence of natural solutions residues in the channels and within the membranes, the RED unit was rinsed with the artificial solutions and conditioned overnight before starting the testing.

Table 3. Typical ion composition (in w/w %) of sea-salt adopted for tests with artificial solutions [a].

Na^+	K^+	Ca^{2+}	Mg^{2+}	Cl^-	SO_4^{2-}
37.7	0.0	0.3	0.8	60.9	0.3
(33-38)	(0-0.5)	(0.2-1.1)	(0.3-2.3)	(57-61)	(0.3-1.6)

[a] The most representative value of concentration is reported for each species, while the typical range of variation is indicated between brackets.

The influence of the dilute feed concentration and flow-rate on process performance was investigated by carrying out the power measurements changing the dilute flow velocity in the range 1 – 1.5 cm/s and conductivity in the range 1.2 – 5.9 mS/cm. Conversely, constant conditions were kept for the concentrate feed, consisting in artificial brine (215 mS/cm) at 1 cm/s flow velocity for all tests. The results of such analysis are reported in Figure 6 in terms of OCV and stack resistance variation.

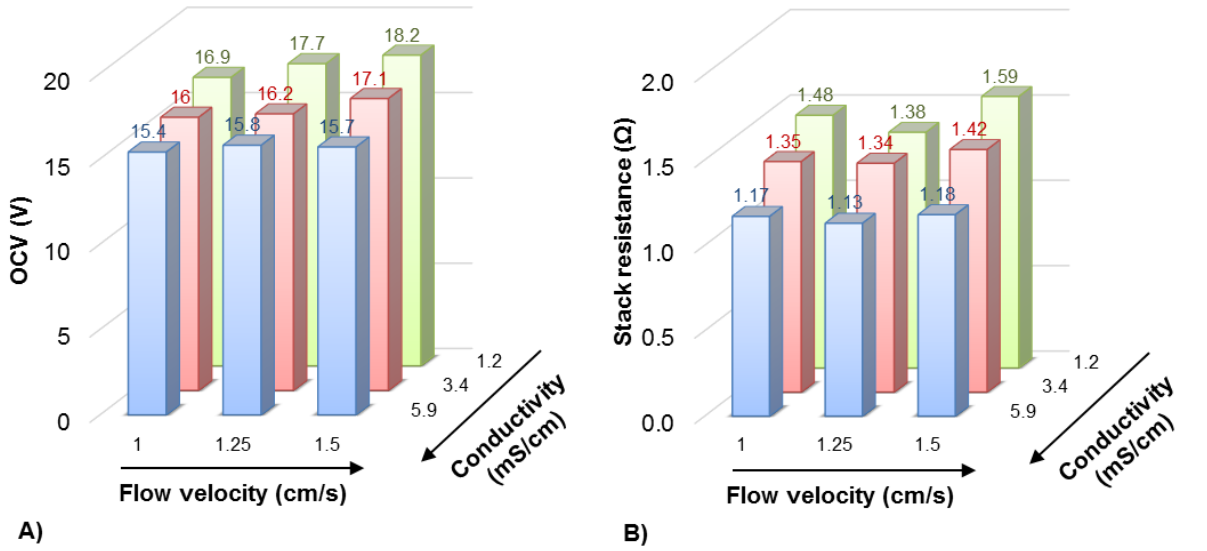

Figure 6. Influence of dilute conductivity and flow rate on OCV (A) and stack resistance (B). Power measurements performed feeding the prototype with artificial brine (NaCl solution at 215 mS/cm, flow velocity 1 cm/s, $T_{HIGH} \approx$ 28 °C) and artificial brackish water (NaCl solution at 1.2 – 5.9 mS/cm, $T_{LOW} \approx$ 25 °C).

The strongest dependence of OCV was observed when increasing the dilute conductivity, leading to a reduction related to the lower salinity gradient available for the process (Figure 6.A). An increase of dilute flow velocity leads to a very slight increase of OCV, though the dependence is so weak to be comparable with experimental error. The opposite dependence was found for the stack resistance (Figure 6.B), which was enhanced by the reduction in the dilute conductivity. No significant dependence was found between the stack resistance and the flow velocity.

The counter-acting effect on OCV and stack resistance is eventually reflected in the power output trends, characterised by a scattering of measured power output values around an average above 50 W (Figure 7). This value is 30-40% higher than that obtained with real solutions, thus indicating a detrimental effect of the use of natural solutions on the system performance.

From Figure 7, it can be noted that the power production in the RED system was stable in a wide range of operating conditions, highlighting only small variation with respect to the average values of power density and with no indication of a sharp value of optimal conductivity or velocity. This evidence is in good agreement with the findings of Tedesco *et al.* [25], who carried out process simulations identifying such relatively wide range of LOW concentrations as an optimal choice for maximising the power output of the system.

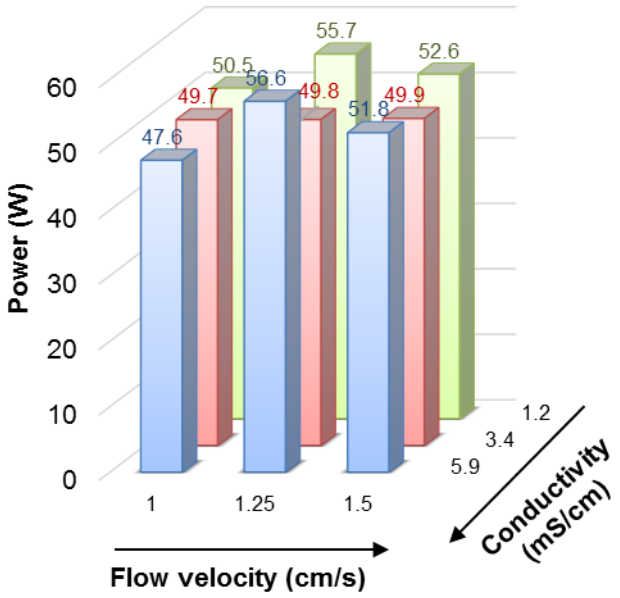

Figure 7. Influence of dilute conductivity and flow rate on power output. Power measurements performed feeding the prototype with artificial brine (NaCl solution at 215 mS/, flow velocity 1 cm/s, $T_{HIGH} \approx 28$ °C) and artificial brackish water (NaCl solution at 1.2 – 5.9 mS/cm, $T_{LOW} \approx 25$ °C).

Although the use of the above mentioned artificial solutions leads to an increase in power output with respect to the case of natural solutions, this is not yet representative of operations with pure-NaCl solutions. In fact, sea-salt from saltworks still contains small amounts of ions different from Na^+ and Cl^- (K^+, Mg^{2+}, SO_4^{2-}), which may have a relevant impact on the performance, though being normally below 3-5% in terms of mass fraction.
For this reason, the RED unit was also tested with artificial solutions prepared with 99.5% pure sodium chloride (SOSALT S.p.A., Italy). The power measurements were performed changing the conductivity of the dilute, ranging from 0.6 up to 5 mS/cm, while the conductivity of the artificial brine was kept close to the saturation point (≈ 210 mS/cm). Results are shown in Figure 8, where the relevant electric variables (stack voltage, resistance, power and power density) are reported as a function of the conductivity of feed dilute solution.

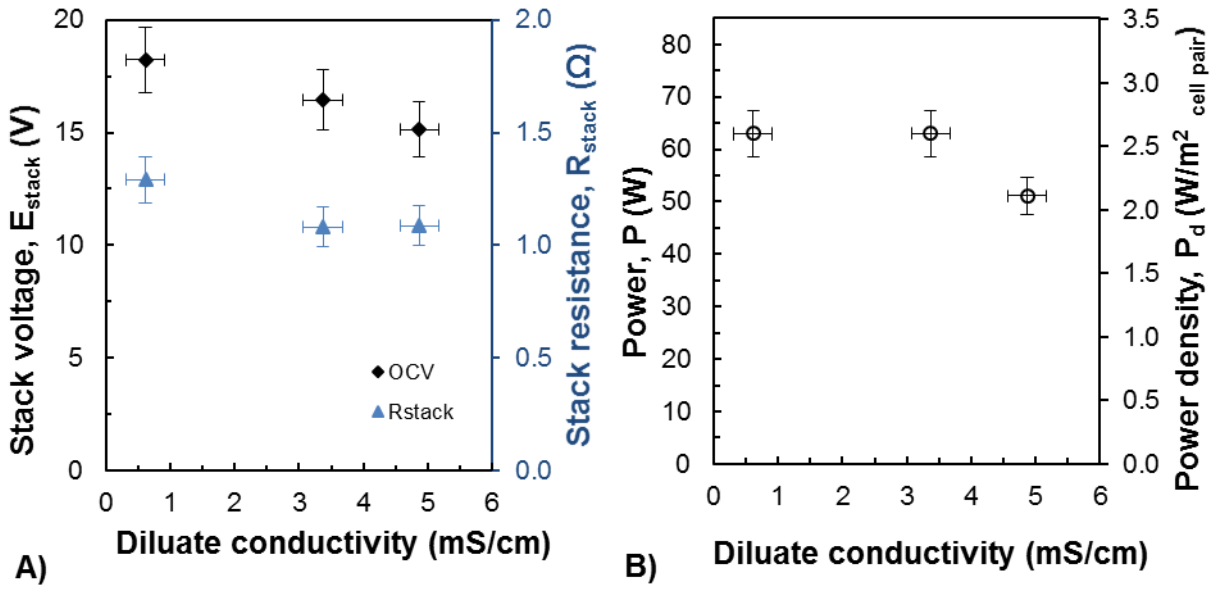

Figure 8. Influence of dilute feed conductivity on process performance. A) Stack voltage and resistance. B) Power and power density. Power measurements performed feeding the prototype with artificial solutions prepared with 99.5% NaCl. Brine conductivity: ~ 210 mS/cm. Flow velocity: ~1 cm/s (8 l/min feed flow rate). T ≈ 23 °C.

In accordance with the previous case (Figure 6), a decrease of stack resistance and OCV is observed when increasing the dilute conductivity (Figure 8.A). As a consequence, a rather constant power output was reached when using 0.6 and 3.4 mS/cm NaCl solutions, while a reduced power was measured at 5 mS/cm (Figure 8.B).
The direct comparison of stack performance with natural and artificial solutions is shown in Figure 9, comparing tests where both dilute and concentrate streams were fed to the stack at 8 l/min flow rate.

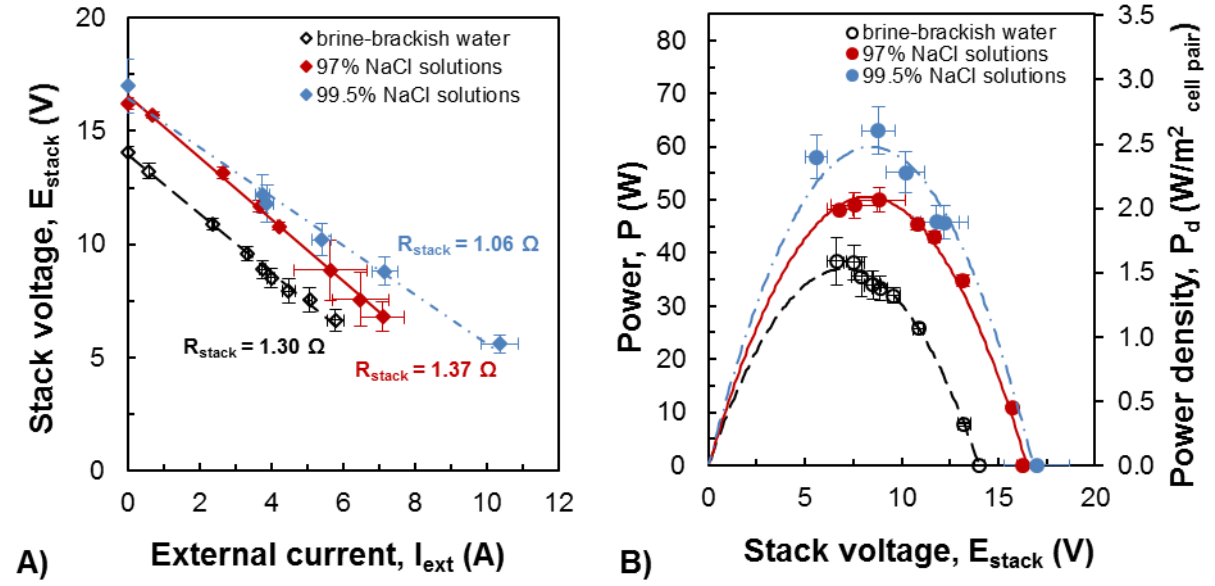

Figure 9. Power measurements performed with real (brackish water - brine) and artificial (sea-salt and 99.5% NaCl) solutions. A) Polarization curve. B) Power and power density curve. Brine conductivity: 196 ± 11 mS/cm. Brackish water conductivity: 3.4 ± 0.1 mS/cm. Flow velocity: 1 cm/s (~8 l/min feed flow rate). T = 25 ± 3 °C.

Significant differences in process performance are observed when feeding the plant with the three different sets of solutions. In particular, the use of real solutions leads to a 13% reduction in the OCV with respect to the case of both artificial solutions with sea-salt (Figure 9.A). This indicates how the presence of significant quantities (up to 40-50% in mols) of non-NaCl ions (e.g. K^+, Ca^{2+}, Mg^{2+}, SO_4^{2-}) reduce the electro-motive force of the membranes pile. This effect might be related to the different activity of salts in the brine and the reduced IEMs permselectivity with non-NaCl salts. Conversely, a lower stack resistance is registered only when passing from the sea-salt to the 99.5% NaCl solutions, thus confirming that even small quantities (3-5%) of non-NaCl ions present in the sea-salt can significantly affect the membrane resistance, as already demonstrated in previous laboratory investigations [23,36,37]. The effect of bivalent ions on RED performance was also investigated by Post et al. [36] and Vermaas et al. [37]. In particular, Veermas et al. performed experimental tests adding 10% $MgSO_4$ to the NaCl feed solutions, observing a power reduction ranging from 29 up to 50% (depending on membrane type [37]).
As a final result, a power output of ~ 65 W was achieved using 99.5% NaCl solutions, thus exceeding a 60-70% increase with respect to the case of real solutions (Figure 9.B).
The use of natural solutions in a real environment remarkably affects the performance of the process. Such findings are in agreement with the outcomes of laboratory investigations reported in the literature [23]. In particular, using artificial brackish water and brine with a salt composition similar to the present case real solutions, Tufa et al. [23] measured a 63% reduction in power density with respect to the reference case adopting artificial solutions. The main effect was attributed to the presence of Mg^{2+} ions, which drastically increase the IEMs resistance.

4.3 Long-term performance of the plant

During the whole experimental campaign, a significant amount of data was collected from May 2014 to September 2014, feeding the system with real brine and brackish water, and then with artificial solutions prepared with sea-salt or pure NaCl. The overall performance of the prototype over five months of operation is shown in Figure 11, where the main performance indicators (gross and net power, yield and efficiency) are reported for the most relevant tests carried out during the experimental campaign.
In most cases, the experimental points reported in Figure 11 are obtained as a mean of 3 different measurements. The reproducibility of the experiments was good, as ±5% discrepancy was normally encountered, when the same feed solution were adopted (i.e. tests performed within the same day). However, the scattering of data shown in Figure 11 is mainly due to the different experimental conditions investigated (e.g. changing flow rate or conductivity), or caused by the variable conditions of the real brine (temperature, conductivity and composition) during the period, or by different operating choices of the experimental campaign (small changes in inlet/outlet channel configurations, inversion of concentrate and dilute channel, etc.). More detailed information on the variables monitored during the tests (conductivity, flow rates and electric variables) is reported in the Appendix.
The power achieved with real brine and brackish water in typical conditions was around 35-40 W (i.e. 1.5-1.7 $W/m^2_{cell\ pair}$), with peak values around 45 W. The net power output oscillated around an average of 25 W, with higher values registered for the artificial solutions and lower values when using the natural brines and saline waters. In particular, Figure 10 reports the observed trend of net power output versus total pressure drops in the HIGH and LOW compartments, indicating how the net power significantly decreased when increasing pressure drops. It is worth noting that the use of natural solutions also affected pressure drops, especially in the HIGH compartment. In one case the operation of the prototype even resulted in a negative net power (-7 W), due to the very high pressure drops occurring in that specific test (flow

velocity of 2.3 cm/s for brackish water and 1.5 cm/s for the brine), despite a gross power output slightly above the average (43 W).

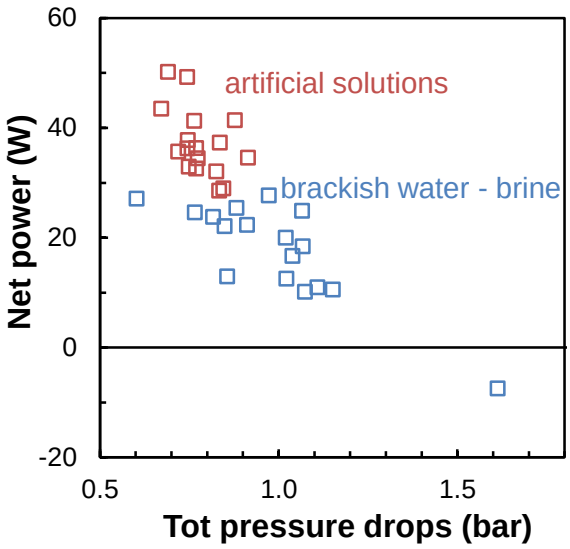

Figure 10. Observed trend of Net Power output versus total pressure drops (intended as a sum of pressure drops in the LOW and the HIGH compartments).

Using NaCl (99.5% pure) artificial solutions the power output increased up to ~ 65 W (2.7 $W/m^2_{cell\ pair}$), which represents the highest value registered during the experimental campaign. The yield of the plant resulted in values from 0.03 up to 0.06 kWh/m^3 of feed solution when operating with natural feed streams, and increased up to 0.1 kWh/m^3 in the case of artificial NaCl solutions. Such finding is in accordance with the efficiency, which reached values in the range of 2-3% for the case of brackish water-brine and up to almost 5% with artificial solutions. These values are relatively lower than those commonly presented for the RED process with fresh water and seawater (realistic prediction by Feinberg *et al.* [38] indicate a range from 10 to 20%). In fact, the use of highly concentrated brine leads to a reduction of the membranes permselectivity [9,39] and, therefore, of the energy efficiency of the process.
Concerning the long term stability of the process, the experimental campaign has demonstrated how the RED prototype has been able to work in a wide range of operating conditions, showing stable performance over the entire period of testing. Interestingly, no significant problems of scaling or fouling were encountered, as indicated by the time-independent performance of the pilot unit.
Further research activities will have to investigate the long-term operations of the RED process (e.g. days or weeks), typical of industrial scale processes.

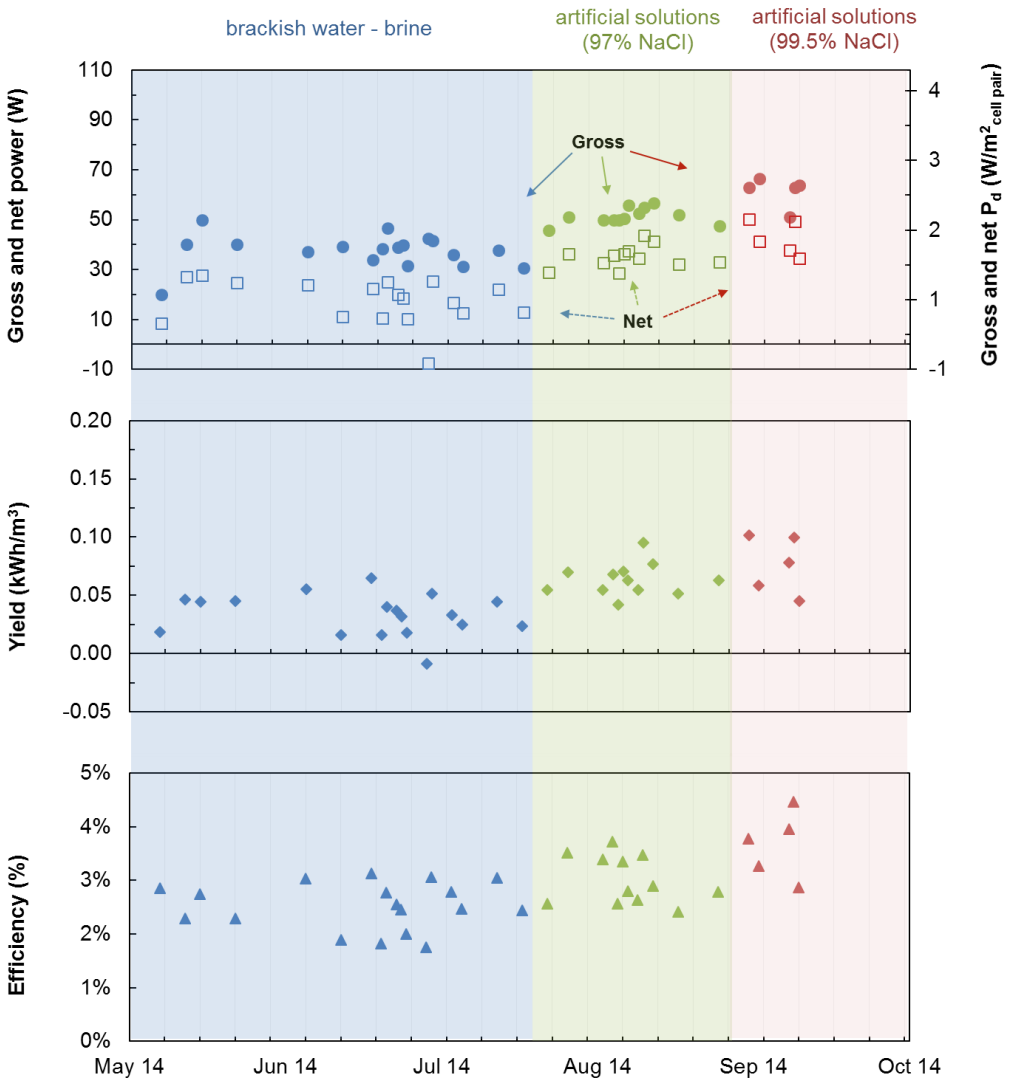

Figure 11. Overall performance of the prototype over five months of operation. Range of variable conditions: brine conductivity: 135 - 220 mS/cm; dilute conductivity: 0.6 - 6mS/cm; temperature: 17-31°C; flow velocity: 0.8 – 2.4 cm/s. More detailed information on the monitored variables during the tests (conductivity, temperature, flow rates and electric variables) are reported in the Appendix (Figure A.1).

5 Conclusions

The installation, commissioning and testing of the first RED pilot plant operating with real brackish water and brine were presented. A RED unit with 44x44 cm^2 membrane area and 125 cell pairs has been tested for five months using natural and artificial solutions. In particular, using real brackish water and concentrated brine as feed solutions, an average power output of 40 W (i.e. 1.6 W/m$^2_{\text{cell pair}}$) was reached. The same RED unit was tested also with artificial solutions, adopted as a reference case for maximum power output of the system. These solutions were prepared either with sea-salt (purity in NaCl 95-97%) and NaCl (purity 99.5%), and their use as feed solutions has led to a significant increase in the power output, achieving values up to 65 W. All these values represent the highest power output reported so far in the literature for reverse electrodialysis systems.

Testing the unit with natural and artificial solutions highlighted how the use of real feed streams can cause a reduction of process performance in the range of 40-50% (in terms of power output). Such reduction is likely due to the presence of relevant amounts of non-NaCl salts, especially Mg^{2+}, in the real solutions.
Interestingly, the RED prototype was tested over a period of five months, operating in a wide range of operating conditions without showing any significant performance loss during the whole experimental campaign. The stable operations were assessed when testing the plant with real solutions as well as with the artificial ones, thus demonstrating for the first time the technological feasibility of the RED process on a pilot-scale and a real operating environment.
A future work will focus on the installation and testing of two larger and further optimised RED units, each one equipped with 500 cell pairs, aiming at reaching a total membrane area installed of more than 400 m^2, with a target power capacity of the plant in the order of 1 kW.

Acknowledgements

This work has been performed within the REAPower (Reverse Electrodialysis Alternative Power production) project, funded by the EU-FP7 programme (Project Number: 256736). Fujifilm and REDstack are acknowledged for providing the membranes and the RED module. The authors are grateful to Maurizio Bevacqua, Carmelo Cirino and Luigi Gurreri for their help during the construction and commissioning of the pilot plant. The valuable support of our technicians, Mr. Giacomo Galante and Mr. Giuseppe Fanale is also warmly and deeply acknowledged.

Nomenclature

A	Membrane area, m^2
C	Molar concentration, mol/m^3
C_{eq}	Equilibrium concentration, mol/m^3
I	External current, A
N	Number of cell pairs, -
OCV	Open circuit voltage, V
P	Electric power, W
E_{stack}	Stack voltage, V
P_d	Power density, W/m^2 of cell pair
$P_{d,net}$	Net power density, W/m^2 of cell pair
P_{net}	Net power, W
P_{rev}	Theoretical power, W
Q	Volumetric flow rate, m^3/s
Q_{av}	Average flow rate of dilute and concentrate, m^3/s
R	Universal gas constant, $J\ mol^{-1}\ K^{-1}$
R_{stack}	Stack electric resistance, Ω
T	System temperature, K
Y	Process yield, kWh/m^3 of average feed flow rate

Greek letters

γ	mean activity coefficient of NaCl, -
Δp	pressure drops, bar
η	energy efficiency, %

η_{pump} pump efficiency, -

Subscripts

HIGH concentrate
LOW dilute

Acronyms and Abbreviations

ERS	Electrode Rinse Solution
RED	Reverse electrodialysis
SGP	Salinity gradient power
E-I	Stack potential *vs* external current curve (also called polarisation curve)

References

[1] A. Daniilidis, R. Herber, D.A. Vermaas, Upscale potential and financial feasibility of a reverse electrodialysis power plant, Appl. Energy. 119 (2014) 257–265.

[2] A.M. Weiner, R.K. McGovern, J.H.L. V, A new reverse electrodialysis design strategy which significantly reduces the levelized cost of electricity, J. Memb. Sci. (2015). doi:10.1016/j.memsci.2015.05.058.

[3] R.E. Pattle, Production of Electric Power by mixing Fresh and Salt Water in the Hydroelectric Pile, Nature. 174 (1954) 660.

[4] J. Jagur-Grodzinski, R. Kramer, Novel process for direct conversion of free energy of mixing into electric power, Ind. Eng. Chem. Process Des. Dev. 25 (1986) 443–449.

[5] J.N. Weinstein, F.B. Leitz, Electric power from differences in salinity: the dialytic battery, Sci. (New York, NY). 191 (1976) 557.

[6] M. Turek, B. Bandura, P. Dydo, Power production from coal-mine brine utilizing reversed electrodialysis, Desalination. 221 (2008) 462–466.

[7] D.A. Vermaas, M. Saakes, K. Nijmeijer, Power generation using profiled membranes in reverse electrodialysis, J. Memb. Sci. 385–386 (2011) 234–242.

[8] J. Veerman, M. Saakes, S.J. Metz, G.J. Harmsen, Reverse electrodialysis: Performance of a stack with 50 cells on the mixing of sea and river water, J. Memb. Sci. 327 (2009) 136–144.

[9] M. Tedesco, E. Brauns, A. Cipollina, G. Micale, P. Modica, G. Russo, et al., Reverse Electrodialysis with saline waters and concentrated brines: a laboratory investigation towards technology scale-up, J. Memb. Sci. 492 (2015) 9–20.

[10] X. Luo, X. Cao, Y. Mo, K. Xiao, X. Zhang, P. Liang, et al., Power generation by coupling reverse electrodialysis and ammonium bicarbonate: Implication for recovery of waste heat, Electrochem. Commun. 19 (2012) 25–28. doi:10.1016/j.elecom.2012.03.004.

[11] B.E. Logan, M. Elimelech, Membrane-based processes for sustainable power generation using water, Nature. 488 (2012) 313–319.

[12] R.D. Cusick, Y. Kim, B.E. Logan, Energy Capture from Thermolytic Solutions in Microbial Reverse-Electrodialysis Cells, Science (80-.). 335 (2012) 1474–1477. doi:10.1126/science.1219330.

[13] O. Scialdone, A. D'Angelo, A. Galia, Energy generation and abatement of Acid Orange 7 in reverse electrodialysis cells using salinity gradients, J. Electroanal. Chem. 738 (2015) 61–68.

[14] J.W. Post, C.H. Goeting, J. Valk, S. Goinga, J. Veerman, H.V.M. Hamelers, et al., Towards implementation of reverse electrodialysis for power generation from salinity gradients, Desalin. Water Treat. 16 (2010) 182–193.

[15] J. Veerman, M. Saakes, S.J. Metz, G.J. Harmsen, Electrical power from sea and river water by reverse electrodialysis: A first step from the laboratory to a real power plant, Environ. Sci. Technol. 44 (2010) 9207–9212.

[16] D.A. Vermaas, D. Kunteng, M. Saakes, K. Nijmeijer, Fouling in reverse electrodialysis under natural conditions, Water Res. 47 (2013) 1289–1298.

[17] D.A. Vermaas, D. Kunteng, J. Veerman, M. Saakes, K. Nijmeijer, Periodic feedwater reversal and air sparging as antifouling strategies in reverse electrodialysis, Environ. Sci. Technol. 48 (2014) 3065–3073.

[18] R.E. Lacey, Energy by reverse electrodialysis, Ocean Eng. 7 (1980) 1–47.

[19] E. Brauns, Towards a worldwide sustainable and simultaneous large-scale production of renewable energy and potable water through salinity gradient power by combining reversed electrodialysis and solar power?, Desalination. 219 (2008) 312–323.

[20] A. Daniilidis, D.A.A. Vermaas, R. Herber, K. Nijmeijer, Experimentally obtainable energy from mixing river water, seawater or brines with reverse electrodialysis, Renew. Energy. 64 (2014) 123–131.

[21] M. Tedesco, A. Cipollina, A. Tamburini, G. Micale, J. Helsen, M. Papapetrou, REAPower: use of desalination brine for power production through reverse electrodialysis, Desalin. Water Treat. 53 (2015) 3161–3169.

[22] M. Tedesco, A. Cipollina, A. Tamburini, W. van Baak, G. Micale, Modelling the Reverse ElectroDialysis process with seawater and concentrated brines, Desalin. Water Treat. 49 (2012) 404–424.

[23] R.A. Tufa, E. Curcio, W. Van Baak, J. Veerman, S. Grasman, E. Fontananova, et al., Potential of brackish water and brine for energy generation by salinity gradient power-reverse electrodialysis (SGP-RE), RSC Adv. 4 (2014) 42617–42623.

[24] M. Tedesco, A. Cipollina, A. Tamburini, I.D.L. Bogle, G. Micale, A simulation tool for analysis and design of reverse electrodialysis using concentrated brines, Chem. Eng. Res. Des. 93 (2015) 441–456.

[25] M. Tedesco, P. Mazzola, A. Tamburini, G. Micale, I.D.L. Bogle, M. Papapetrou, et al., Analysis and simulation of scale-up potentials in reverse electrodialysis, Desalin. Water Treat. 55 (2015) 3391–3403.

[26] A. Cipollina, A. Misseri, G.D. Staiti, A. Galia, G. Micale, O. Scialdone, Integrated production of fresh water, sea salt and magnesium from sea water, Desalin. Water Treat. 49 (2012) 390–403.

[27] E. Fontananova, W. Zhang, I. Nicotera, C. Simari, W. Van Baak, G. Di Profio, et al., Probing membrane and interface properties in concentrated electrolyte solutions, J. Memb. Sci. 459 (2014) 177–189.

[28] J. Veerman, M. Saakes, S.J. Metz, G.J. Harmsen, Reverse electrodialysis: Evaluation of suitable electrode systems, J. Appl. Electrochem. 40 (2010) 1461–1474.

[29] O. Scialdone, C. Guarisco, S. Grispo, A.D. Angelo, A. Galia, Investigation of electrode material - Redox couple systems for reverse electrodialysis processes. Part I: Iron redox couples, J. Electroanal. Chem. 681 (2012) 66–75.

[30] O. Scialdone, A. Albanese, A.D. Angelo, A. Galia, C. Guarisco, Investigation of electrode material - Redox couple systems for reverse electrodialysis processes. Part II: Experiments in a stack with 10–50 cell pairs, J. Electroanal. Chem. 704 (2013) 1–9.

[31] D.A. Vermaas, J. Veerman, N.Y. Yip, M. Elimelech, M. Saakes, K. Nijmeijer, High efficiency in energy generation from salinity gradients with reverse electrodialysis, ACS Sustain. Chem. Eng. 1 (2013) 1295–1302.

[32] X. Zhu, W. He, B.E. Logan, Reducing pumping energy by using different flow rates of high and low concentration solutions in reverse electrodialysis cells, J. Memb. Sci. 486 (2015) 215–221. doi:10.1016/j.memsci.2015.03.035.

[33] P. Długołęcki, P. Ogonowski, S.J. Metz, M. Saakes, K. Nijmeijer, M. Wessling, On the resistances of membrane, diffusion boundary layer and double layer in ion exchange membrane transport, J. Memb. Sci. 349 (2010) 369–379.

[34] D.A. Vermaas, M. Saakes, K. Nijmeijer, Doubled Power Density from Salinity Gradients at Reduced Intermembrane Distance, Environ. Sci. Technol. 45 (2011) 7089–7095.

[35] S. Pawlowski, P. Sistat, J.G. Crespo, S. Velizarov, Mass transfer in reverse electrodialysis: Flow entrance effects and diffusion boundary layer thickness, J. Memb. Sci. 471 (2014) 72–83.

[36] J.W. Post, H.V.M. Hamelers, C.J.N. Buisman, Influence of multivalent ions on power production from mixing salt and fresh water with a reverse electrodialysis system, J. Memb. Sci. 330 (2009) 65–72.

[37] D.A. Vermaas, J. Veerman, M. Saakes, K. Nijmeijer, Influence of multivalent ions on renewable energy generation in reverse electrodialysis, Energy Environ. Sci. 7 (2014) 1434–1445.

[38] B.J. Feinberg, G.Z. Ramon, E.M.V. Hoek, Scale-up characteristics of membrane-based salinity-gradient power production, J. Memb. Sci. 476 (2015) 311–320. doi:10.1016/j.memsci.2014.10.023.

[39] A. Daniilidis, D.A. Vermaas, R. Herber, K. Nijmeijer, Experimentally obtainable energy from mixing river water, seawater or brines with reverse electrodialysis, Renew. Energy. 64 (2014) 123–131.

[40] B.R. Staples, Activity and Osmotic Coefficients of Aqueous Alkali Metal Nitrites, J. Phys. Chem. Ref. Data. 10 (1981) 765–777.

[41] G. Jones, C.F. Bickford, The conductance of aqueous solutions as a function of the concentration. I. Potassium bromide and lanthanum chloride, J. Am. Chem. Soc. 56 (1934) 602–611.

Appendix

A.1 Estimation of activity coefficients and equivalent conductivities

Activity coefficients were estimated according to the correlation proposed by Staples [40]:

$$\ln \gamma = \frac{-|z_+ z_-| A_\gamma \, m^{1/2}}{1 + B_\gamma \, m^{1/2}} + C_\gamma \, m + D_\gamma \, m^2 + E_\gamma \, m^3 \tag{A.1}$$

where A_γ = 1.17625 $kg^{1/2}$ $mol^{-1/2}$, m is the molality of the solution, z_+ and z_- are the cation and anion valence numbers, respectively. The coefficients B_γ, C_γ, D_γ, E_γ are function of the nature of the electrolyte, and their values for NaCl are reported in Table A.1.

Table A.1. Parameters of Staples' correlation (eq. A.1).

Salt	B_γ	C_γ	D_γ	E_γ
Sodium Chloride	1.2751	0.0956	5.82E-05	0.0005

The equivalent conductivity is estimated by means of Jones and Dole's equation [41]:

$$\Lambda = \Lambda_0 - \frac{A_\Lambda \, c^{1/2}}{1 + B_\Lambda \, c^{1/2}} - C_\Lambda \, C \tag{A.2}$$

where Λ_0 is the equivalent conductivity of salt at infinite dilution, c is the molar concentration. The values of model parameters A_Λ, B_Λ, C_Λ for NaCl are reported in Table A.2. Therefore, the molar concentration was estimated as:

$$C_{NaCl} = \frac{\sigma^{\exp}}{\Lambda} \tag{A.3}$$

where σ^{exp} is the value of the experimentally measured conductivity.

Table A.2. Parameters of Jones and Dole' correlation (eq. A.2).

Salt	Λ_0 *	A_Λ	B_Λ	C_Λ
Sodium Chloride	126.5000	91.0239	1.6591	6.8041

A.2 Monitored variables

The RED demonstration plant was tested over a period of five months, changing feed solutions (natural or artificial) and with variable operating conditions (in terms of flow rates, temperatures and conductivities).

The performance of the plant has been evaluated through the figures of merit shown in Figure 10. In addition, Figure A.1 reports all the variables (i.e. conductivity, temperature, flow rates and electric variables) monitored during the experimental campaign.

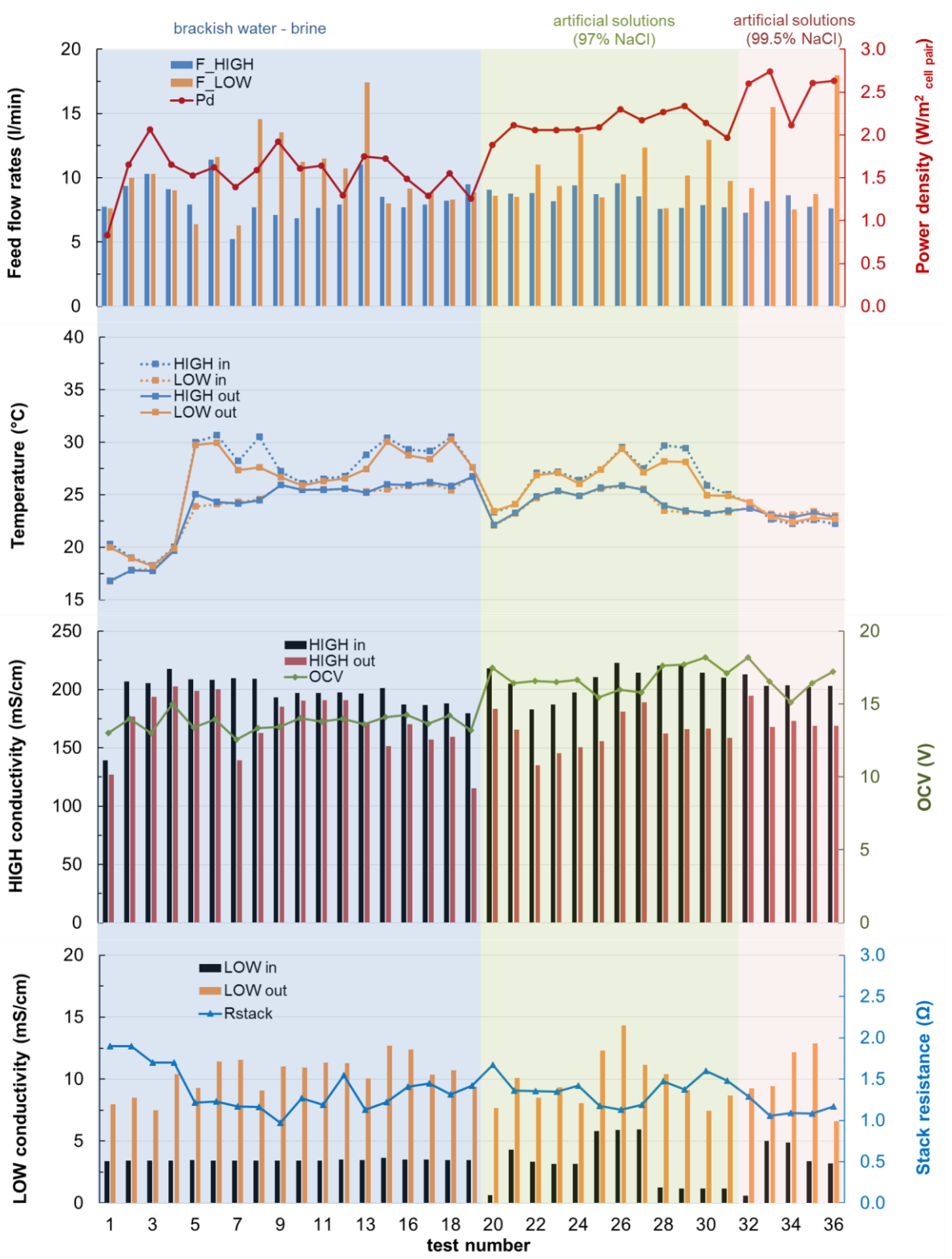

Figure A.1. Overview of the performed tests with the RED prototype (44x44 cm^2, 125 cell pairs) over five months of operation. Range of variable conditions: brine conductivity: 135 - 220 mS/cm; dilute conductivity: 0.6 - 6 mS/cm; temperature: 17-31°C; flow velocity: 0.8 – 2.4 cm/s.